hNET AS A TARGET FOR NEUROBLASTOMA NANOMEDICINE

MARKETA CHAROUSOVA[1,2], SIMONA DOSTALOVA[1,2], YAZAN HADDAD[1,2], VLADISLAV STRMISKA[1,2], SONA KRIZKOVA[1,2], DAVID HYNEK[1,2], VEDRAN MILOSAVLJEVIC[1,2], VOJTECH ADAM[1,2], ZBYNEK HEGER[1,2]

[1] Department of Chemistry and Biochemistry
Mendel University in Brno
Zemedelska 1, 613 00 Brno
[2] Central European Institute of Technology
Brno University of Technology
Purkynova 123, 612 00 Brno
CZECH REPUBLIC

charousovam@gmail.com

Abstract: Chemotherapy often results in various side effects, which can negatively affect health. Neuroblastoma, one of the most common types of childhood cancer, is but one of the examples, where side effects of chemotherapeutic treatment lower the quality of patient's life. Modern way how to fight that is to enclose cytotoxic drug into some nanocarrier and its targeting to receptors overexpressed in membranes of cancer cells. Apoferritin (Apo), a natural protein cage, is very suitable as a nanocarrier, as it has no toxicity, immune system does not react to it, and drug can easily be loaded into its cavity. We enclosed ellipticine, clinical tested anti-cancer drug, into Apo cavity (creating ApoElli). The percentage of encapsulation was 61% and size and transmission electron microscopy analysis showed the preserved Apo ~12 nm icosahedral structure after this encapsulation. Then we modified Apo outer surface with *in silico*-modelled peptides with hNET affinity and tested its toxicity and hemolytic activity. ApoElli modified with anti-hNET peptides was able to internalize into neuroblastoma cells and to deliver the drug. However, it proved to be safe for human RBC, unlike pure ellipticine, which caused observable hemolysis at the same concentration.

Key Words: ellipticine; hemolysis; nanoconstruct; neuroblastoma; toxicity

INTRODUCTION

Neuroblastoma is the most common cancer among children; the average age of diagnosis is 17 month (Davenport et al. 2012). This cancer is arising in adrenal medulla or paraspinal ganglia and affects development of sympathetic nervous system. Over 50% of tumours are present in abdomen, neck, chest or pelvis (Vo et al. 2014). It is well known for its wide variety of clinical behaviour depending on the site of primary tumour, presence or absence of metastatic disease sites etc. (Park et al. 2010). Diagnosis is performed by INSS (International Neuroblastoma Staging System), whose criteria were first formulated in 1986 (Brodeur et al. 1993). Initial tests include CT or MRI to evaluate primary tumour, localize it, and define its size and possible spreading. Pathological confirmation is performed from biopsy of tumour tissue or from neuroblastoma tumour cells in bone marrow sample (Park et al. 2010). Treatment methods include surgery, chemotherapy, radiotherapy and biotherapy, as well as observation with selected circumstances (Maris et al. 2007). Approved drugs for neuroblastoma are for example doxorubicin hydrochloride, vincristine sulphate, Clafen®, Cytoxan® or CEM®. Side effects of chemotherapeutic drugs can be very serious; some of them might appear years after successful treatment, such as 65% of childhood patients treated with doxorubicin hydrochloride who suffer from its cardiotoxicity in adulthood (Hutchins et al. 2017).

One way how to protect organism against these side effects is to close these drugs into some nanocarrier. For this experiment, apoferritin (Apo) was selected. It is a regular, uniformly self-assembling nano-sized protein cage with excellent biocompatibility and unique structure that allows encapsulation of small molecules into its inner core (Belletti et al. 2017). It has many positive

characteristics, the mechanism of drug loading can be based on passive penetration process through pores (Linder 2013) or active pH-dependent disassembly/reassembly protocol (Dostalova et al. 2017). Apo has a long lifetime and has affinity for tumour cells, though it has the ability to bind at human TfR1 receptor, which is over-expressed in rapidly proliferating cells (Li et al. 2010).

Apo surface can be further modified (Blazkova et al. 2013) and so can be directed to different cell types which increases its specificity. In this paper, we modified Apo surface with gold nanoparticles and use them to further modify the surface with peptides with high affinity for human norepinephrine transporter (hNET). The affinity of various peptide sequences for this receptor was tested using homology modelling (Haddad et al. 2017), and two different peptides were chosen for *in vitro* studies. This modification allowed to increase the Apo specificity and allow transport into cells through norepinephrine transporter receptor overexpressed on the membranes of neuroblastoma cells (Haddad et al. 2017).

The ability to deliver drug molecules to neuroblastoma cells was tested using ellipticine (Elli). It is an alkaloid that was first isolated from *Ochrosia elliptica*. Preclinical and clinical studies showed that ellipticine has ability to arrest growth of several cancer cell types (Poljakova et al. 2009), but has multiple toxic side effects, including hemotoxicity (Auclair 1987). The mechanism of action has not been precisely described , but it combines DNA damage by inhibition of topoisomerase II, generation of cytotoxic free radicals, regulation of Bcl-2 family protein, rescue of mutant p53 activity and initiation of mitochondrial apoptosis pathway (Kuo et al. 2005). However Elli is a possible mutagen (Stiborova et al. 2001) and has no specificity, so can also eliminate healthy cell. To protect healthy cells from effects of Elli and also specify place of toxic effect, we encapsulated Elli into Apo creating ApoElli.

MATERIAL AND METHODS

Chemicals

All chemicals of ACS purity were obtained from Sigma-Aldrich (St. Louis, MO, USA), unless stated otherwise. The pH was measured using pH meter WTW inoLab (Weilheim, Germany).

Encapsulation of Elli into Apo and modification of its surface with hNET peptides

200 µl of 1 mg/ml Elli (dissolved in 150 : 1 1 M HCl) was added to 20 µl of 50 mg/ml horse spleen Apo and 100 µl of ACS water. The solution was mixed for 15 min. 0.66 µl of 1 M sodium hydroxide was added to increase the pH and encapsulate the Elli inside Apo (creating ApoElli). The solution was mixed for 15 min. To remove non-encapsulated Elli molecules, solution exchange was performed three times (6000 g and 4 °C for 15 min). 25 µl of 1.3 nm gold nanoparticles was added to the sample and the solution was mixed for 12 h, creating ApoElli+Au. To remove unbound gold nanoparticles, solution exchange was performed two times. Next, 2.8 µl of 1.25 mg/ml anti-hNET peptide A (GASNGINAYLC, creating ApoElli+hNET pA) or anti-hNET peptide B (SLWERLAYGIC, creating ApoElli+hNET pB) was added to the sample. The sample was mixed for 1 h at 600 rpm and 45 °C. Solution exchange was performed two times to remove unbound peptide molecules. Samples were stored at 4 °C until used.

Characterization of nanocarrier

To evaluate Elli concentration in ApoElli and its encapsulation efficiency, absorbance at wavelength of 420 nm and fluorescence with excitation wavelength of 420 nm and emission wavelength of 450 nm were measured using Tecan Infinite 200 PRO (Tecan, Männendorf, Switzerland).

The average size of the nanocarrier was determined by quasielastic dynamic light scattering with Zetasizer Nano ZS instrument (Malvern Instruments Ltd., Worcestershire, UK). The nanocarrier was diluted with ACS water (1 : 200), placed into polystyrene latex cell and measured at a detector angle of 173°, wavelength of 633 nm and temperature of 25 °C with the refractive index of dispersive phase 1.45 and 1.333 for the dispersive environment. For each measurement, disposable cuvettes type ZEN0040, were used, containing 50 µl of sample. The equilibration time was 120 s. The measurements were performed in hexaplicates.

Visualization of the nanocarrier shape was performed using transmission electron microscopy (TEM) with negative staining technique. For this purpose, an organotungsten compound, Nano-W (Nanoprobes, Yaphank, NY, USA) was utilized. 4 µl of samples was deposited onto 400-mesh cooper grids coated with a continuous carbon layer. Dried grids were imaged by TEM (Tecnai F20; FEI, Hillsboro, OR, USA).

Toxicity of peptides and nanocarrier

MTT toxicity test were performed with neuroblastoma cell lines NB4, and SH-SY5Y to evaluate the cytotoxicity of anti-hNET peptides A and B (in concentration range of 0.98-1000 µM), Elli, ApoElli, ApoElli+hNET pA and ApoElli+hNET pB (in Elli concentration range of 0.078-80 µM). 5000 cells in 50 µl of medium were seeded in each well of 96-well plate. The cells were incubated at 37 °C for at least 8 h. 50 µl of samples diluted in culture medium was added to cells, with one well receiving only culture medium. The plates were incubated at 37 °C for 12 h, after which 10 µl of 5 mg/ml of MTT (3-(4,5-dimethylthiazol-2-yl)-2,5-diphenyltetrazolium bromide) dissolved in PBS (pH 7.4; 0.137 M NaCl + 0.0027 M KCl + 0.0014 M KH_2PO_4 + 0.0043 M Na_2HPO_4), was added to every well. After further incubation at 37 °C for 3 h, the solution was removed and 100 µl of dimethylsulfoxide was added to disrupt the cells and release purple formazan. Absorbance of the samples at 570 nm was measured by Tecan Infinite 200 PRO.

Hemolytic assay was performed to evaluate hemotoxicity of Apo, Elli, ApoElli, ApoElli+hNET pA and ApoElli+hNET pB). Fresh blood is centrifuged at 3000 rpm for 10 min. Blood plasma was removed and red blood cells (RBCs) were repeatedly washed by 150 mM sodium chloride and centrifuged at 3000 rpm for 10 min, until supernatant cleared from haemolytic RBCs. After that, the RBCs were diluted with PBS and 150 µl was mixed with 150 µl of various concentrations (0.0468-0.375 mM) of the tested Elli nanoformulations. PBS was used as negative control and 0.1% Triton X-100 was used as positive control. All samples were incubated at 37 °C for 1 h and centrifuged at 3000 rpm for 10 min. Absorbance of 50 µl supernatant at 540 nm was measured using Tecan Infinite 200 PRO. The percentage of hemolysis was calculated using formula:

$$\%\text{hemolysis} = [(A_t - A_c)/(A_{100\%} - A_c)] \cdot 100 \quad (1)$$

A_t stands for absorbance of supernatant from sample, A_c represents absorbance of supernatant from negative control and $A_{100\%}$ stands for absorbance of supernatant from positive control.

RESULTS AND DISCUSSION

Table 1 Average size of the tested nanocarriers

Sample	Average size (nm)
Apo	12.0
ApoElli	15.7
ApoElli+hNET pA	18.2
ApoElli+hNET pB	43.8

Average Elli encapsulation efficiency into Apo was 61%, as evaluated by absorbance measurement. The average size of the nanoparticles was measured to further confirm the surface modifications (Table 1). While the average size of empty Apo is ~12 nm, encapsulation of Elli increased it to 15.7 nm. This could be caused by less rigid assembly after filling of the cavity or by drug molecules attached to the outer surface of the nanocarrier. Modification with anti-hNET peptide A increased the size to an average of 18.2 nm, proving that if there were drug molecules on the outer surface, their presence did not hamper binding of targeting peptides. The biggest size, around 43.8 nm, was measured for ApoElli modified with anti-hNET peptide B. Since during the homology modelling the peptide B was found to bind to other peptide B molecules, this was probably caused by formation of multiple ApoElli connected by these peptides.

Figure 1 TEM visualization, A –Apo; B – ApoElli; C – ApoElli +Au, arrow shows Au nanoparticles, D – ApoElli+hNET pA, arrows show visible peptide tails E – ApoElli+hNET pB, arrows show visible peptide tails

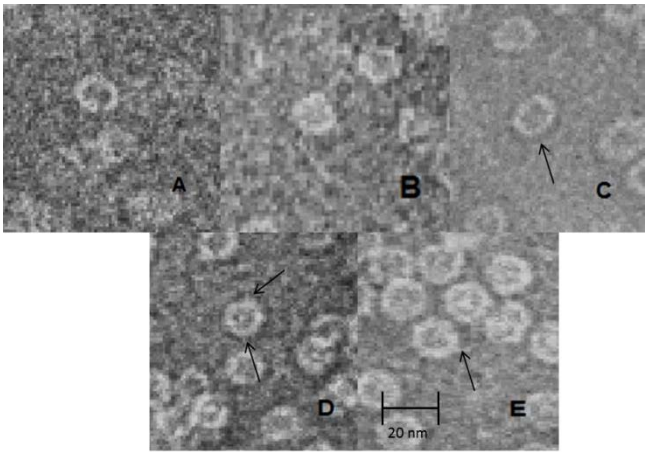

To evaluate the structure of nanoparticles, TEM visualization was used (Figure 1). The structure of unloaded Apo (Figure 1A) shows icosahedral cage with empty cavity. On the next picture is Apo loaded with Elli (Figure 1B, ApoElli) where a filled cavity can be clearly observed. Gold nanoparticles on ApoElli surface can be seen as a dark ring around ApoElli (arrow on Figure 1C, ApoElli+Au). Peptides present on the surface of ApoElli+hNET pA and ApoElli+hNET pB were observed as small protein tails on the icosahedral cage (arrows on Figures 1D and 1E, respectively). However, all pictures showed typical apoferritin structure in its stable and assembled state, proving that the performed surface modifications did not lead to disassembly of its structure.

Table 2 MTT toxicity test

Cell line	Sample	$24IC_{50}$ (μM)
SH-SY5Y	anti-hNET peptide A	330.0
	anti-hNET peptide B	203.0
	Elli	8.8
	Apo	ND
	ApoElli	16.5
	ApoElli+hNET pA	16.5
	ApoElli+hNET pB	20.7
NB4	anti-hNET peptide A	ND
	anti-hNET peptide B	216.0
	Elli	7.3
	Apo	ND
	ApoElli	16.3
	ApoElli+hNET pA	16.2
	ApoElli+hNET pB	15.5

To evaluate the cytotoxicity of these nanocarriers for neuroblastoma cells, MTT toxicity test was performed using two different neuroblastoma cell lines, SH-SY5Y and NB4. The peptides themselves proved non-toxic for these neuroblastoma cells lines, where their $24IC_{50}$ was 30 fold higher than that used for ApoElli targeting. Empty Apo was did not show any toxicity. Samples containing Elli reached $24IC_{50}$ at low dosage, and encapsulated Elli reached $24IC_{50}$ with concentration 2.5 fold higher than pure Elli. These results show that Apo nanocarrier was able to deliver Elli cargo to cells, where its structure was disassembled due to acidic endosomal environment and Elli was released.

Figure 2 Hemolysis test; Letter describe samples, A – Apo, B – Elli, C – ApoElli, D – ApoElli+hNET pA, E – ApoElli+hNET pB, graph shows percentage of hemolysis by highest concentration of samples

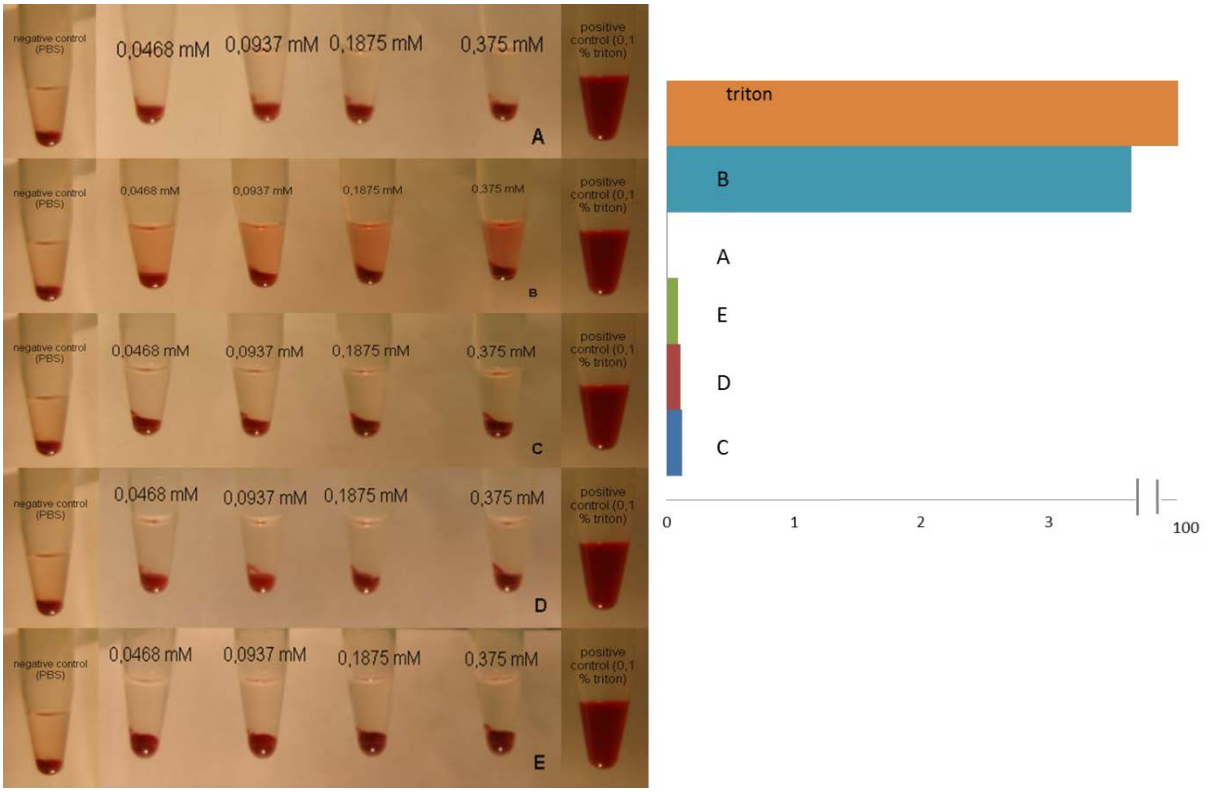

Hemolytic test was performed using fresh RBCs. 0.1% Triton was used as a positive control, as it hemolysed 100% of RBCs. PBS was used as a negative control. Empty Apo had no hemolytic effect at all (Figure 2A). Pure Elli caused observable hemolysis, as it hemolysed 3.6% of RBCs at its highest concentration (Figure 2B). Elli encapsulated into Apo (Figure 2C) and its modifications with anti-hNET peptides A (Figure 2D) and B (Figure 2E) were not hemolytic for RBCs. Percentage of hemolysis caused by these nanoformulations was below 1% at all tested concentrations. It can be seen, that ApoElli with peptide B was a little less hemolytic then ApoElli and ApoElli with peptide A.

CONCLUSION

We managed to create possible nanocarrier loaded with anti-cancer drug ellipticine. By closing Elli into this protein carrier Apo we can protect healthy cells as with modification of Apo surface we are able to specifically target it to cancer cells. In this paper we encapsulated Elli into Apo and modified its outer surface with gold nanoparticles and anti-hNET peptide A and hNET peptide B for neuroblastoma targeting. We characterized the size and structure of these particles and proved that these modifications did not affect the structure of Apo and so its function. We also demonstrated safety of this nanocarrier by itself, but also when loaded with Elli and modified with targeting peptides. Elli itself proved toxic for both cancer and red blood cells, even in low concentration. Whereas the encapsulation in Apo keeping the toxicity for neuroblastoma cancer cells while eliminating the toxicity for red blood cells, although the highest concentration applied to red blood cells was almost 25 fold higher than that used on neuroblastoma cancer cells. By modifying of Apo surface, we proved that the transport of cytotoxic drug with many side effects can be more specific to affect only target cancer cells. Still, further experiments are needed to evaluate the targeting and *in vivo* behaviour of this nanocarrier.

ACKNOWLEDGEMENTS

The research was financially supported by the Grant Agency of the Czech Republic (GA CR 17-12816S) and CEITEC 2020 (LQ1601).

REFERENCES

Auclair, C. 1987. Multimodal Action of Antitumor Agents on DNA - The Ellipticine Series. *Archives of Biochemistry and Biophysics*, 259(1): 1–14.

Belletti, D., Pederzoli, F., Forni, F., Vandelli, M.A., Tosi, G., Ruozi, B. 2017. Protein cage nanostructure as drug delivery system: magnifying glass on apoferritin. *Expert Opinion on Drug Delivery*, 14(7): 825–840.

Blazkova, I., Nguyen, H.V., Dostalova, S., Kopel, P., Stanisavljevic, M., Vaculovicova, M., Stiborova, M., Eckschlager, T., Kizek, R., Adam, V. 2013. Apoferritin Modified Magnetic Particles as Doxorubicin Carriers for Anticancer Drug Delivery. *International Journal of Molecular Sciences*, 14(7): 13391–13402.

Brodeur, G.M., Pritchard, J., Berthold, F., Carlsen, N.L.T., Castel, V., Castleberry, R.P., Debernardi, B., Evans, A.E., Favrot, M., Hedborg, F., Kaneko, M., Kemshead, J., Lampert, F., Lee, R.E.J., Look, A.T., Pearson, A.D.J., Philip, T., Roald, B., Sawada, T., Seeger, R.C., Tsuchida, Y., Voute, P.A. 1993. Revisisons of the International Criteria for Neuroblastoma Diagnosis, Staging, and Response to Treatment. *Journal of Clinical Oncology*, 11(8): 1466–1477.

Davenport, K.P., Blanco, F.C., Sandler, A.D. 2012. Pediatric Malignancies Neuroblastoma, Wilm's Tumor, Hepatoblastoma, Rhabdomyosarcoma, and Sacroccygeal Teratoma. *Surgical Clinics of North America*, 92(3): 745–767.

Dostalova, S., Vasickova, K., Hynek, D., Krizkova, S., Richtera, L., Vaculovicova, M., Eckschlager, T., Stiborova, M., Heger, Z., Adam, V. 2017. Apoferritin as an ubiquitous nanocarrier with excellent shelf life. *International Journal of Nanomedicine*, 12: 2265–2278.

Haddad, Y., Heger, Z., Adam, V. 2017. Targeting Neuroblastoma Cell Surface Proteins: Recommendations for Homology Modeling of hNET, ALK, and TrkB. *Frontiers in Molecular Neuroscience*, 10: 1–4.

Hutchins, K.K., Siddeek, H., Franco, V.I., Lipshultz, S.E. 2017. Prevention of cardiotoxicity among survivors of childhood cancer. *British Journal of Clinical Pharmacology*, 83(3): 455–465.

Kuo, P.L., Hsu, Y.L., Chang, C.H., Lin, C.C. 2005. The mechanism of ellipticine-induced apoptosis and cell cycle arrest in human breast MCF-7 cancer cells. *Cancer Letters*, 223(2): 293–301.

Li, L., Fang, C.J., Ryan, J.C., Niemi, E.C., Lebron, J.A., Bjorkman, P.J., Arase, H., Torti, F.M., Torti, S.V., Nakamura, M.C., Seaman, W.E. 2010. Binding and uptake of H-ferritin are mediated by human transferrin receptor-1. *Proceedings of the National Academy of Sciences of the United States of America*, 107(8): 3505–3510.

Linder, M.C. 2013. Mobilization of Stored Iron in Mammals: A Review. *Nutrients*, 5(10): 4022–4050.

Maris, J.M., Hogarty, M.D., Bagatell, R., Cohn, S.L. 2007. Neuroblastoma. *Lancet*, 369(9579): 2106–2120.

Park, J.R., Eggert, A., Caron, H. 2010. Neuroblastoma: Biology, Prognosis, and Treatment. *Hematology-Oncology Clinics of North America*, 24(1): 65–86.

Poljakova, J., Eckschlager, T., Hrabeta, J., Hrebackova, J., Smutny, S., Frei, E., Martinek, V., Kizek, R., Stiborova, M. 2009. The mechanism of cytotoxicity and DNA adduct formation by the anticancer drug ellipticine in human neuroblastoma cells. *Biochemical Pharmacology*, 77(9): 1466–1479.

Stiborova, M., Bieler, C.A., Wiessler, M., Frei E. 2001. The anticancer agent ellipticine on activation by cytochrome P450 forms covalent DNA adducts. *Biochemical Pharmacology*, 62(12): 1675–1684.

Vo, K.T., Matthay, K.K., Neuhaus, J., London, W.B., Hero, B., Ambros, P.F., Nakagawara, A., Miniati, D., Wheeler, K., Pearson, A.D.J., Cohn, S.L., Dubois, S.G. 2014. Clinical, Biologic, and Prognostic Differences on the Basis of Primary Tumor Site in Neuroblastoma: A Report From the International Neuroblastoma Risk Group Project. *Journal of Clinical Oncology*, 32(28): 3169–3176.